Supplementary Materials for JCI Insight 2018; 3(23):e124297

AAV CRISPR editing rescues cardiac and muscle function for 18 months in dystrophic mice

Chady H. Hakim[1, 2 †], Nalinda B. Wasala[1 †], Christopher E. Nelson[3, 4], Lakmini P. Wasala[1], Yongping Yue[1], Jacqueline A. Louderman[1], Thais B. Lessa[1], Aihua Dai[1], Keqing Zhang[1], Gregory J. Jenkins[1], Michael E. Nance[1], Xiufang Pan[1], Kasun Kodippili[1], N. Nora Yang[2], Shi-jie Chen[5, 6], Charles A. Gersbach[3, 4, 7], Dongsheng Duan[1, 8, 9, 10]

[†], CHH and NBW contributed equally to this work

Correspondence to

Dongsheng Duan Ph.D.
Department of Molecular Microbiology and Immunology
The University of Missouri School of Medicine
One Hospital Dr. M609, MSB, Columbia, MO 65212
Phone: 573-884-9584; Fax: 573-882-4287
Email: duand@missouri.edu

Content

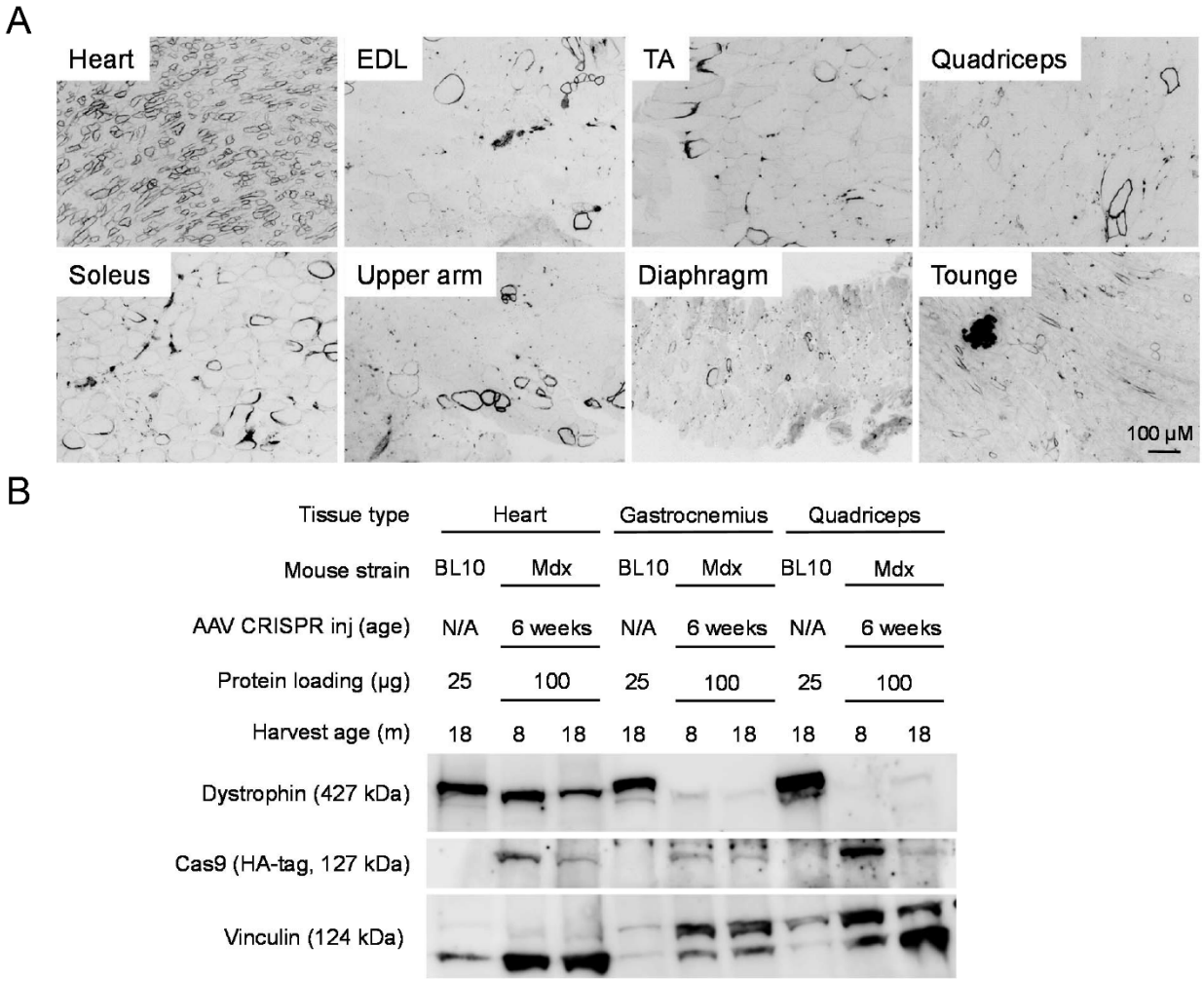

Fig. S1. Evaluation of dystrophin expression at 8 and 18 months in study #1. Six 6-week-old male mdx mice received intravenous injection of the Cas9 vector (7.2 x 10^{12} vg /mouse) and the gRNA vector (3.6 x 10^{12} vg/mouse). One mouse was harvested at 8 months of age and remaining were harvested at 18 months of age. **A,** Representative muscle and heart dystrophin immunostaining photomicrographs from the mouse harvested at 8 months of age. EDL, extensor digitorum longus; TA, tibialis anterior. **B,** Representative dystrophin and Cas9 western blot from the heart, gastrocnemius and quadriceps from the mouse harvested at 8 months of age and a mouse harvested at 18 months of age. Tissue from an 18-month-old BL10 mouse was used as the wild type control. Vinculin served as the loading control. N/A, no AAV injection.

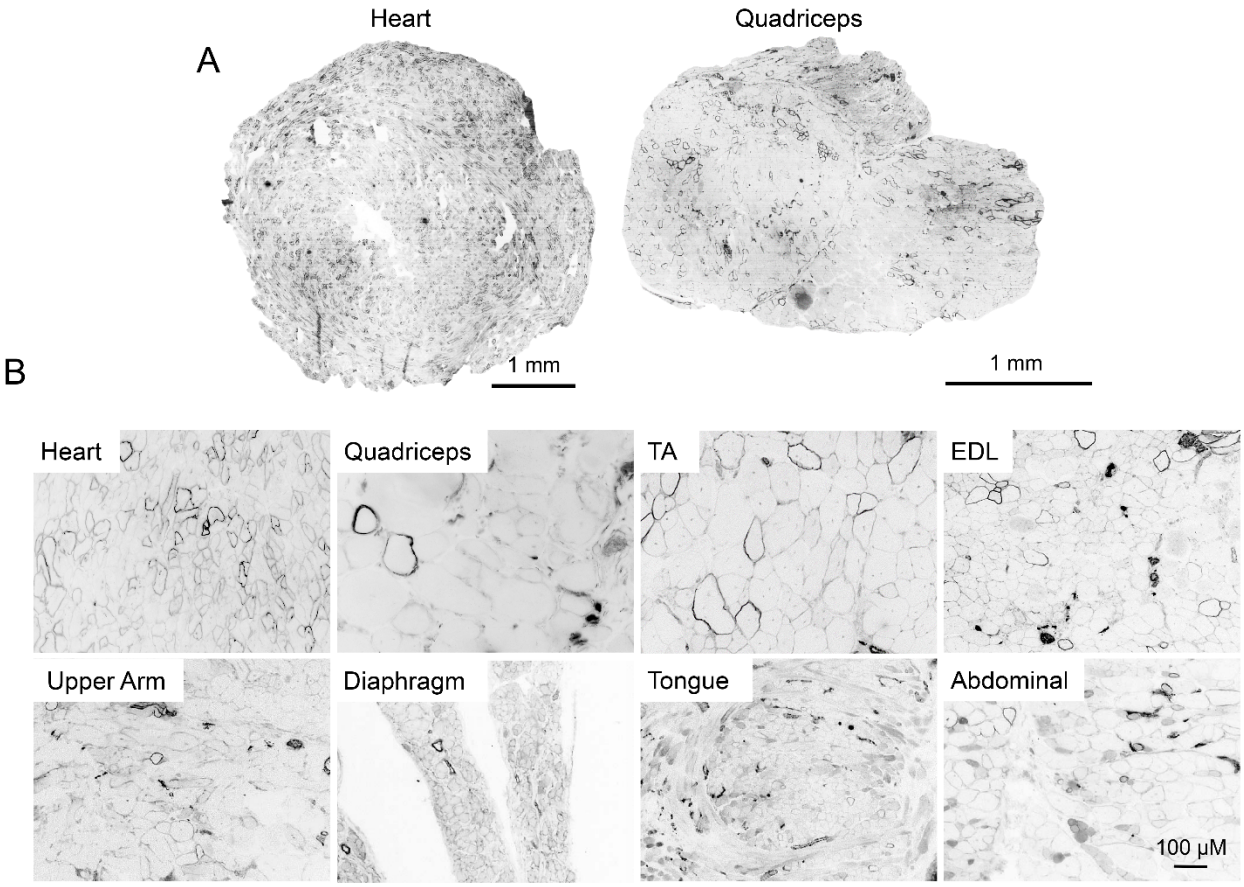

Fig. S2. Representative dystrophin immunofluorescence staining images from a mouse harvested at 18 months in study #1. A, Representative full-view dystrophin staining images of the heart and quadriceps. **B,** Representative high power dystrophin staining images from the heart, quadriceps, tibialis anterior (TA), extensor digitorum longus (EDL), upper arm muscle, diaphragm, tongue and abdominal muscle.

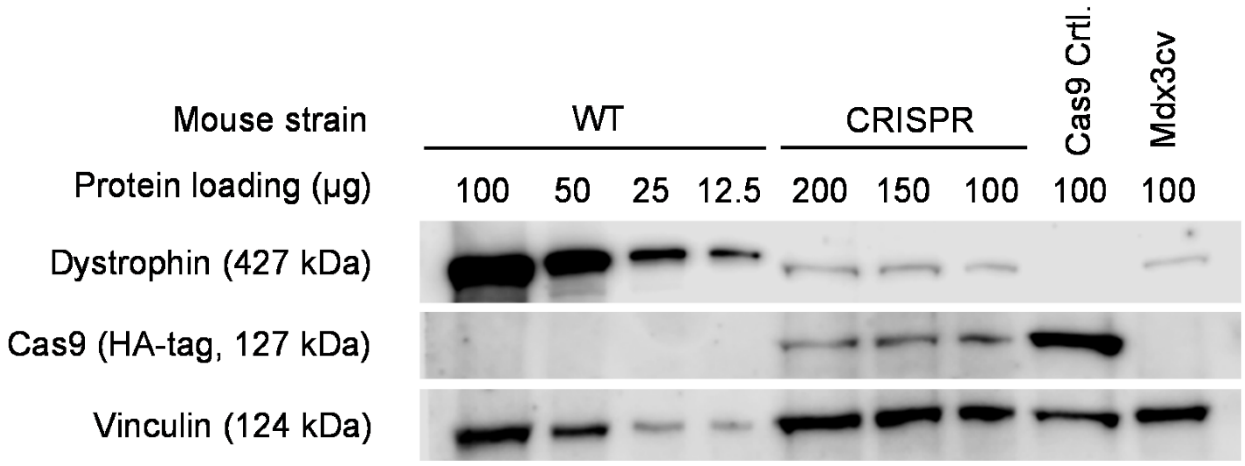

Fig. S3. Titration of dystrophin expression on western blot. Representative dystrophin western blot from the heart of an 18-m-old BL10 mouse (WT), the heart of a study #1 mouse harvested at 18 months of age (CRISPR), the tibialis anterior muscle of a 3-m-old mdx mouse that received local Cas9 AAV vector injection at 6 weeks of age (Cas9 control), and the heart of an 18-m-old mdx3cv mouse. Mdx3cv mouse heart expresses a near full-length dystrophin at ~3.3% of the wild type level (Wasala et al *Journal of Molecular and Cellular Cardiology* 102:45-52, 2017). Vinculin served as the loading control.

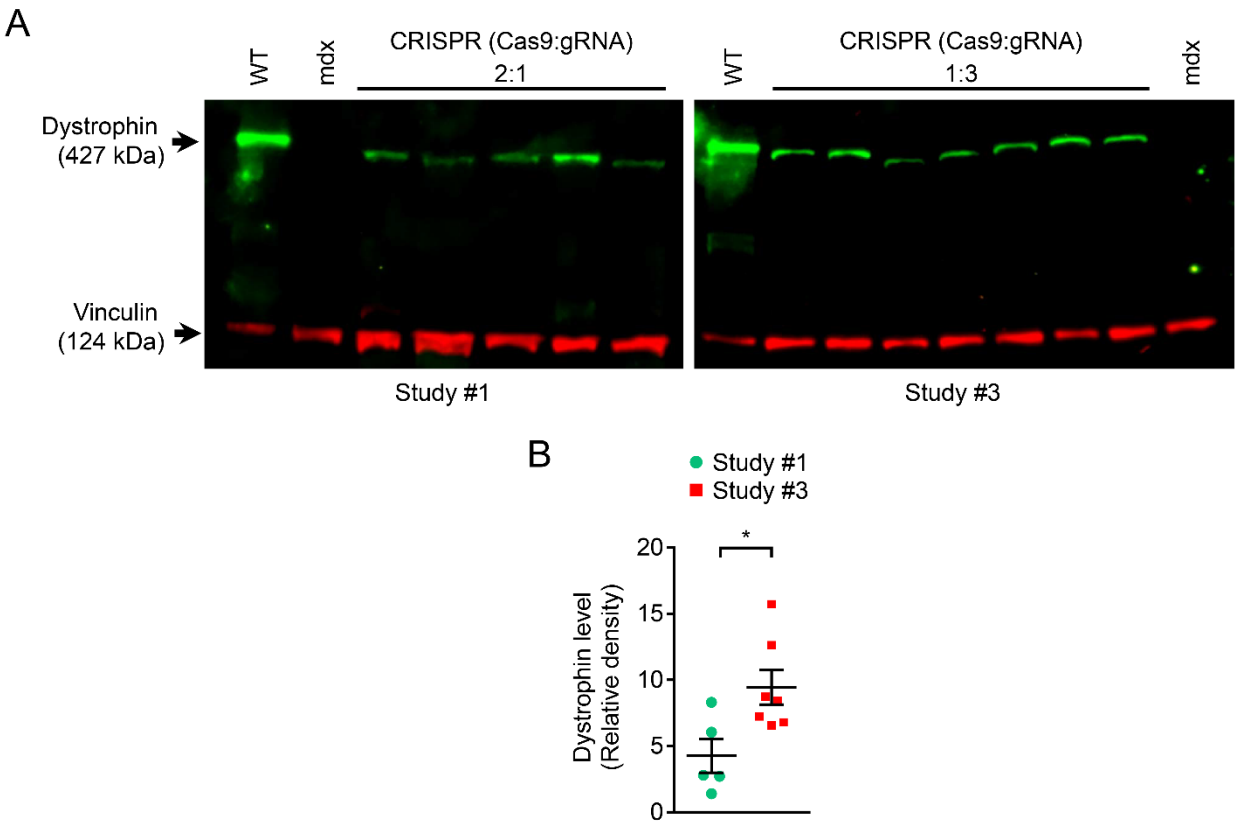

Fig. S4. Quantification of dystrophin restoration in the heart by two-color western blot. To validate chemiluminescence western blot results, we performed LICOR two-color infrared fluorescence western blot using heart lysates collected at 18 months of age from studies #1 and #3. **A**, Western blot images. Heart lysates from BL10 and mdx mice were included as positive and negative controls, respectively. The loading of the BL10 lane was one-fourth of the other lanes. N/A, no AAV injection. **B**, Western blot quantification results. The dystrophin level obtained using the infrared fluorescence detection method was similar to that obtained using the chemiluminescence detection method in Figures 1 and 3. Statistics was done using two tailed Student's t-test. Asterisk, statistically significant ($p<0.05$).

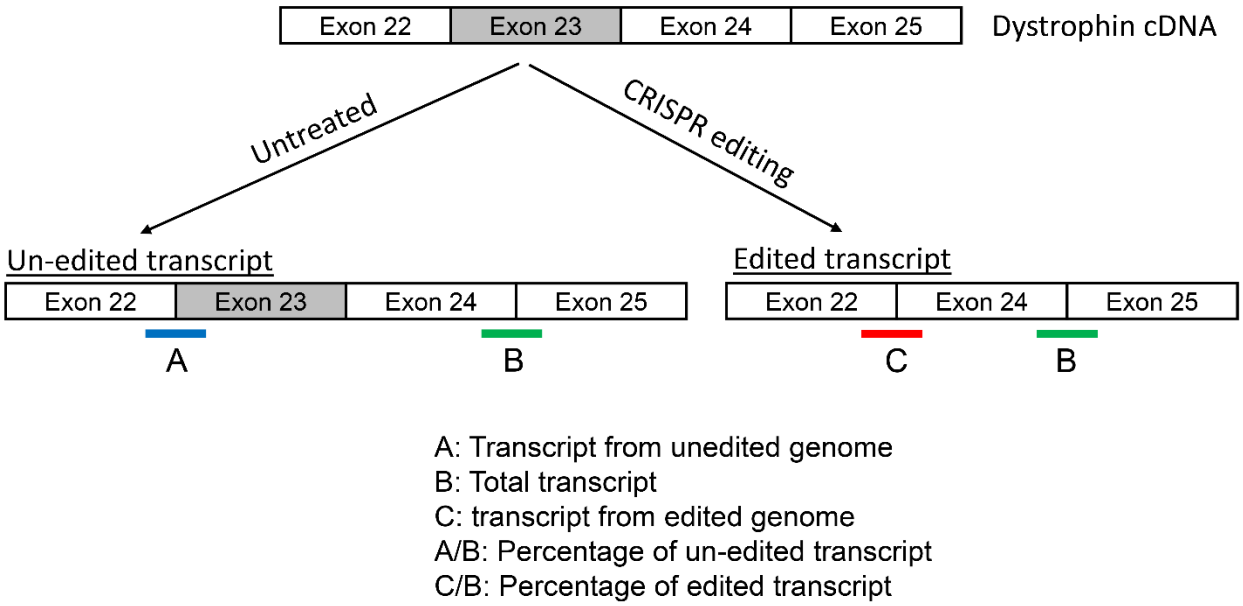

Fig. S5. Schematic outline of the strategy used to quantify dystrophin transcript. The mdx mouse has a nonsense mutation in the exon 23 of the dystrophin gene. In our CRISPR therapy, the mutated exon 23 and its surrounding intronic sequences are removed from the mutated gene. The resulting transcript does not contain exon 23. To detect unedited and edited transcripts, PCR experiments were designed to amplify the junctions of exons 22-23 (*product A* in the figure) and exons 22-24 (*product C* in the figure), respectively. The exons 24-25 junction (*product B* in the figure) was used as the internal control for all dystrophin transcripts (both edited and unedited). In untreated mdx mice, we expect *product B= product A*. CRISPR treated mdx mice have both edited and unedited transcripts. We expect *product B= product A + product C*. The percentage of the edited dystrophin transcript was calculated using the formula: (*product C*)/(*product B*). The percentage of the unedited dystrophin transcript is calculated using the formula: (*product A*)/(*product B*). Exon 23 is shaded to indicate mutation.

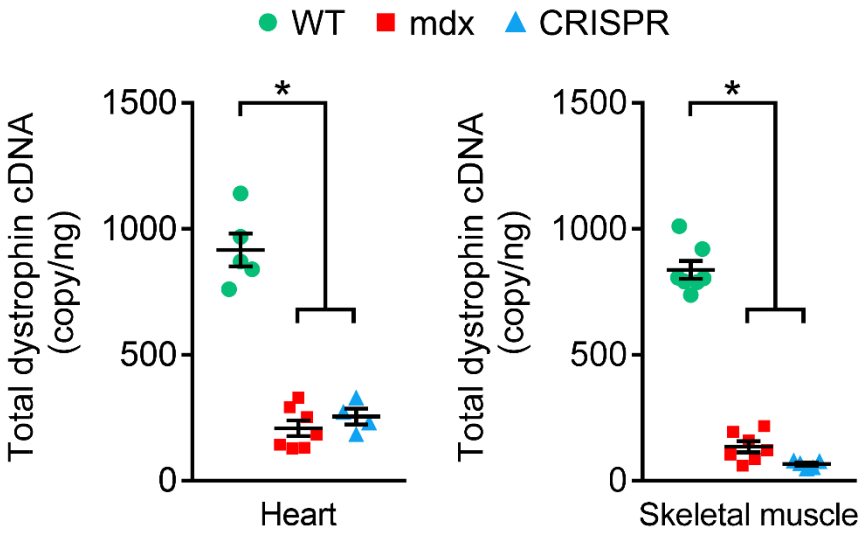

Fig. S6. Quantification of the total dystrophin transcript in study #1. Digital droplet PCR was used to quantify the dystrophin cDNA copy number in the heart and skeletal muscle in 18-m-old mice. Five BL10 mice (WT) and seven untreated mdx mice were used as controls. The total dystrophin transcript in mdx mice was significantly lower than that in wild type mice due to nonsense-mediated decay of the mutated dystrophin transcript (Kerr et al *Human Genetics* 109:402-407, 2011). Statistical analysis was performed using one-way ANOVA. Asterisk, statistically significant ($p<0.05$).

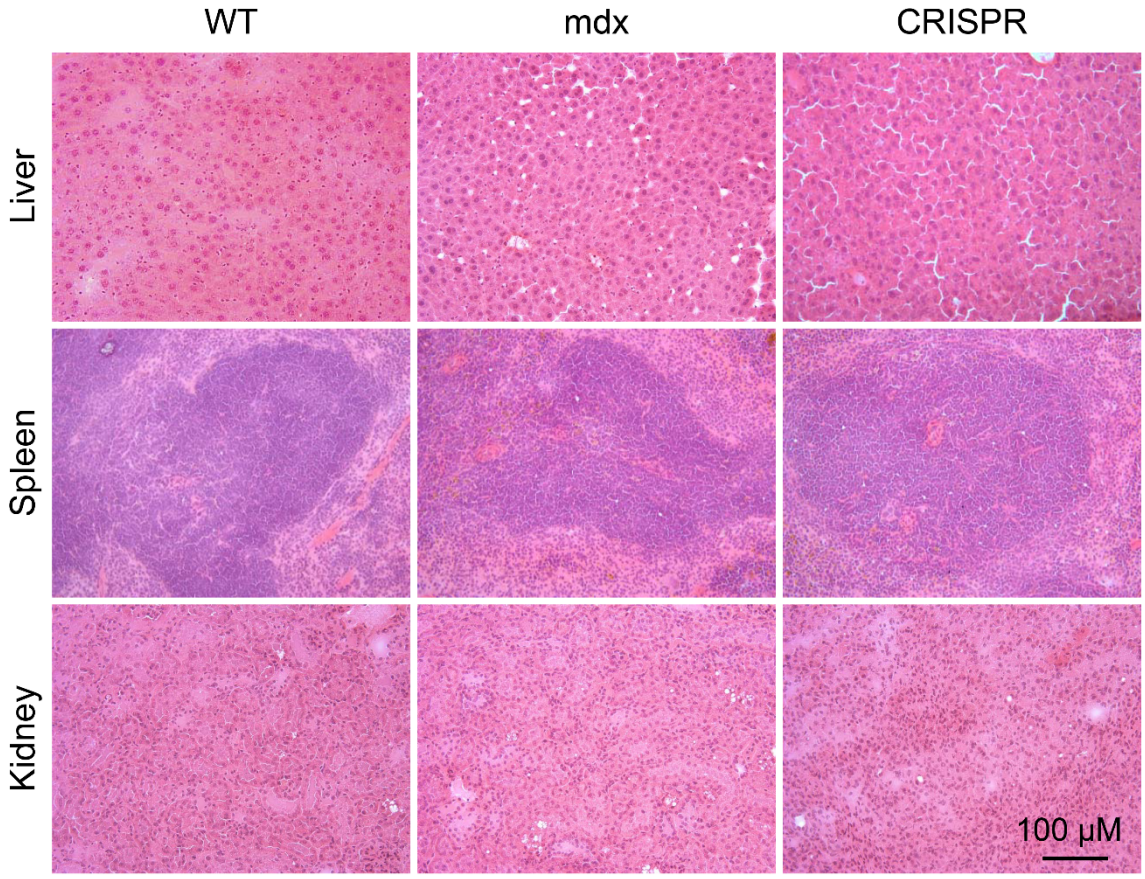

Fig. S7. Histological evaluation of the liver, spleen and kidney in study #1. No obvious abnormalities were detected among wild type (WT), mdx and CRISPR treated mdx mice.

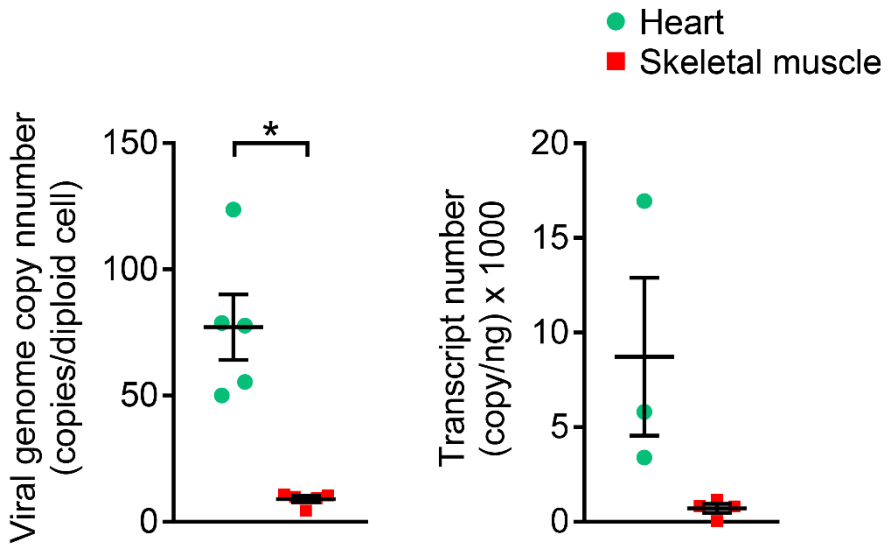

Fig. S8. Quantification of the Cas9 AAV genome copy number and Cas9 transcript at 18 months in study #1. The Cas9 AAV genome copy number was determined by TaqMan PCR. The Cas9 cDNA copy number was determined by digital droplet PCR (n=5 for each group in viral genome copy number analysis and n=3 for heart and n=4 for skeletal muscle in the transcript number analysis). Mann-Whitney test was used for statistical comparison. Asterisk, statistically significant ($p<0.05$).

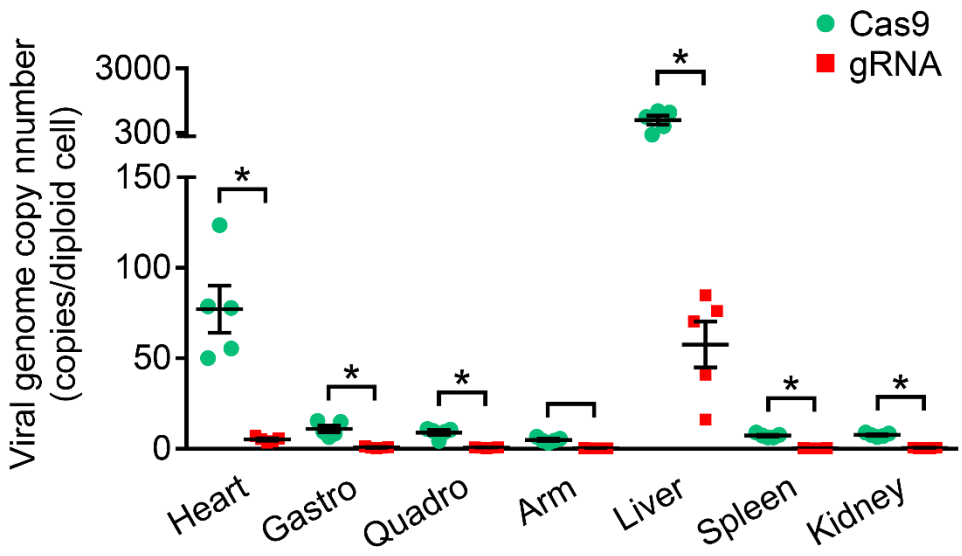

Fig. S9. AAV genome copy number quantification at 18 months in study #1. TaqMan PCR was performed on DNA extracted from the heart, gastrocnemius, quadriceps, arm muscle, liver, spleen and kidney (n=5 for each tissue). In all the tissues examined, the genome copy number of the Cas9 vector was significantly higher than that of the gRNA vector. Multiple t-test was used to determine the statistical significance. Asterisk, statistically significant ($p<0.05$).

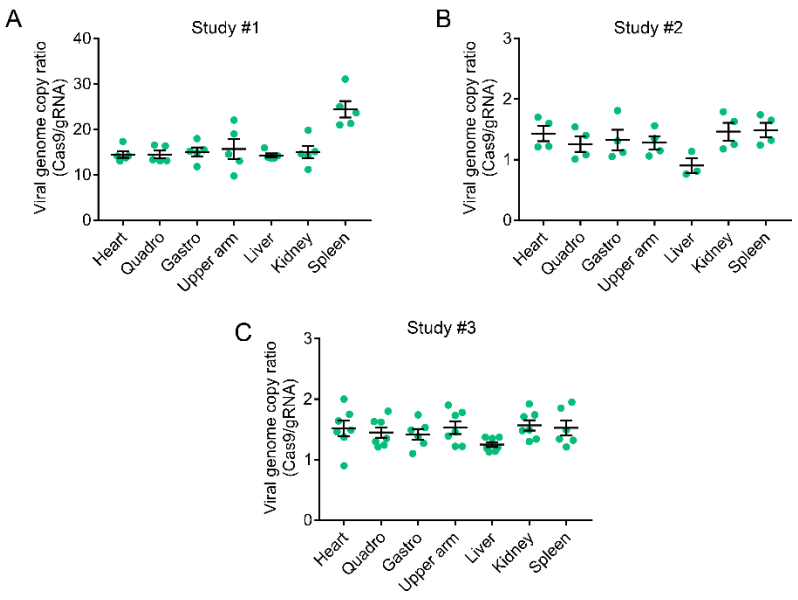

Fig. S10. The Cas9 to gRNA vector genome copy number ratio at 18 months in studies #1-3. The Cas9 to gRNA vector genome copy number ratios were calculated for the heart, quadriceps, gastrocnemius, upper arm muscle, liver, kidney and spleen in all three studies indicated in Table S1. **A,** The results from mice harvested at 18 months of age in study #1. **B,** The results from study #2. **C,** The results from study #3. In study #1, the Cas9 vector and the gRNA vector were delivered at 6 weeks of age at a ratio of 2:1. In studies #2 and 3, the Cas9 vector and the gRNA vector were delivered at 6 weeks of age at a ratio of 1:3. Since the Cas9 vector and the gRNA vector were packaged in the same viral capsid (AAV-9), we expected them to yield a similar transduction efficiency. In other words, the amount of the Cas9 and the gRNA vector genome that reached to the nucleus should be proportional to the amount of the vector administered at the time of injection. If the genome of the Cas9 and gRNA vector had the similar stability, we would expect the ratio of the Cas9 to gRNA vector genome in tissues to be similar to that of injection. However, we found a ratio of ~12-14 in tissues collected from study #1 and a ratio of ~1-1.5 in tissues collected from studies #2 and 3. This far exceeded the expected ratios of 2 (for

study #1) and 0.33 (for studies #2 and 3). Our results suggest a selective depletion of the gRNA vector genome.

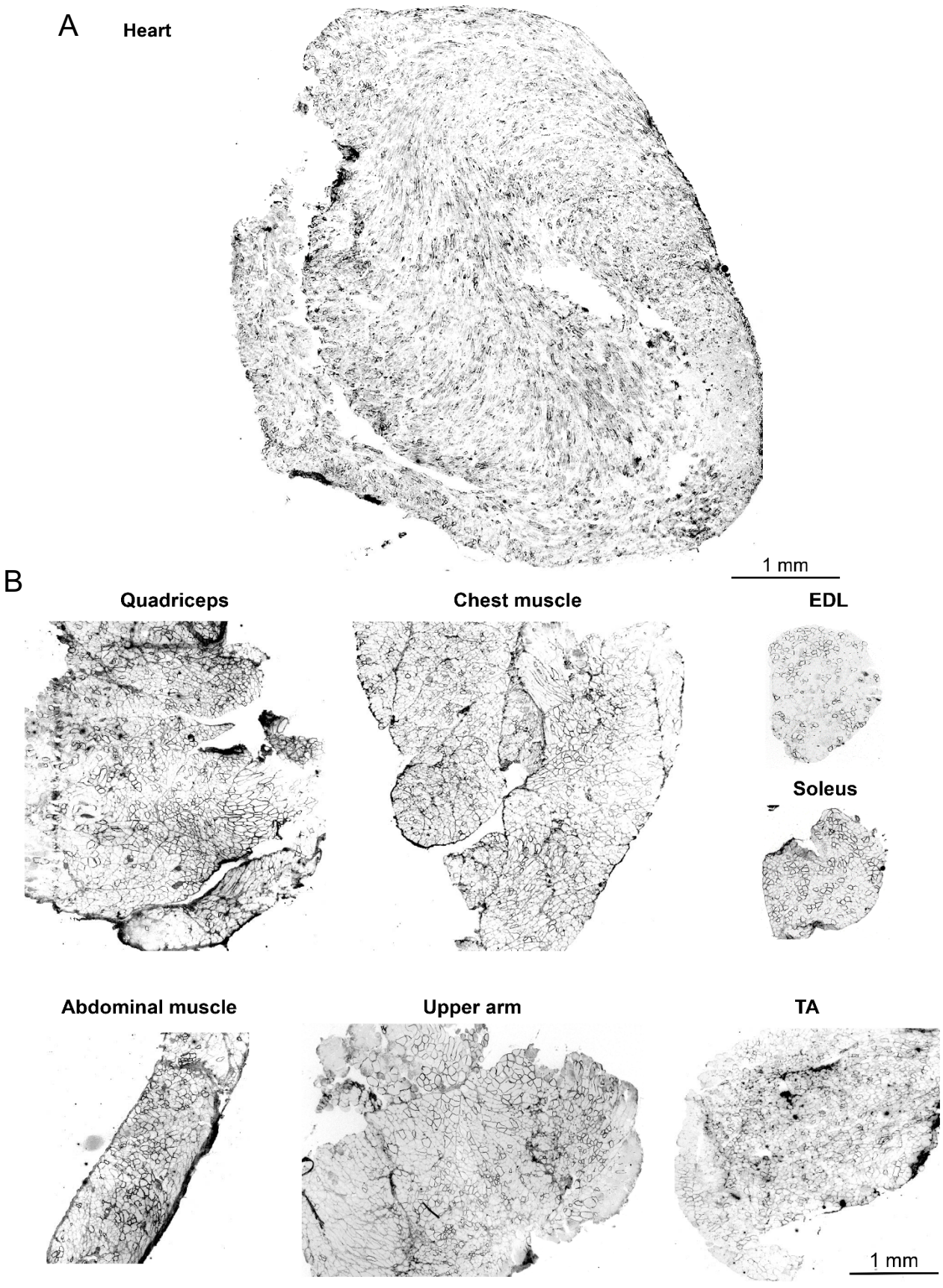
A
Heart
1 mm
B
Quadriceps
Chest muscle
EDL
Soleus
Abdominal muscle
Upper arm
TA
1 mm

Fig. S11. Representative dystrophin immunofluorescence staining images in study #2. A, Representative full-view dystrophin staining images of the heart. **B,** Representative high power dystrophin staining images from the quadriceps, chest muscle, extensor digitorum longus (EDL), tibialis anterior (TA), abdominal muscle (Abd), soleus and upper arm muscle.

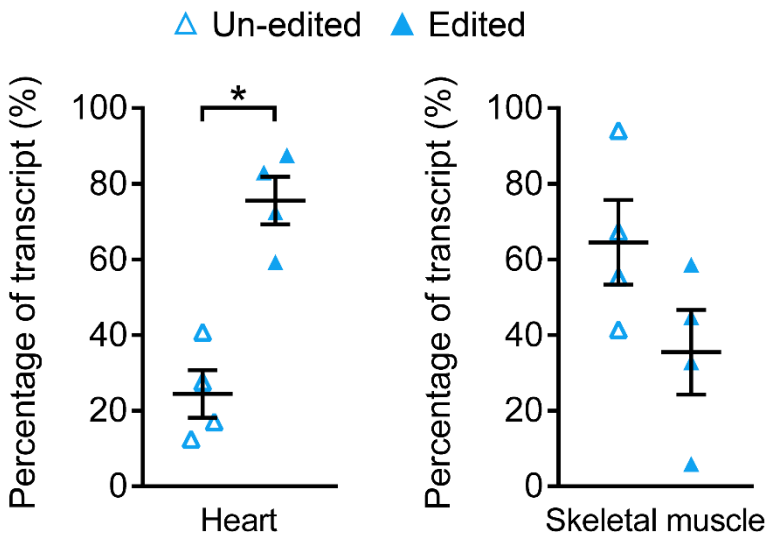

Fig. S12. Quantification of the edited and unedited dystrophin transcripts in study #2. Digital droplet PCR was used to quantify the copy number of edited and unedited dystrophin transcripts in the heart and skeletal muscle from study #2 mice (n=4 for each tissue). Statistical analysis was performed using Mann-Whitney test. Asterisk, statistically significant ($p<0.05$).

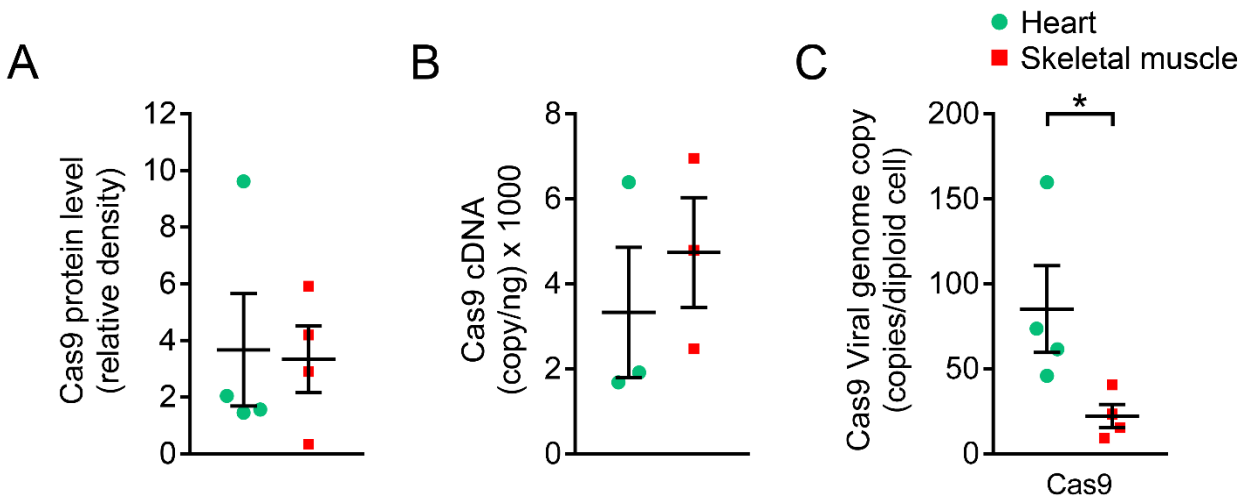

Fig. S13. Evaluation of Cas9 protein, Cas9 transcript and Cas9 AAV genome copy number in study #2. The Cas9 protein was examined by quantitative western blot. The Cas9 cDNA copy number was determined by digital droplet PCR. The Cas9 AAV genome copy number was determined by TaqMan PCR. (n=4 for each tissue for A and C and n=3 for each tissue in B). Statistical analysis was done using Mann-Whitney test. Asterisk, statistically significant ($p<0.05$).

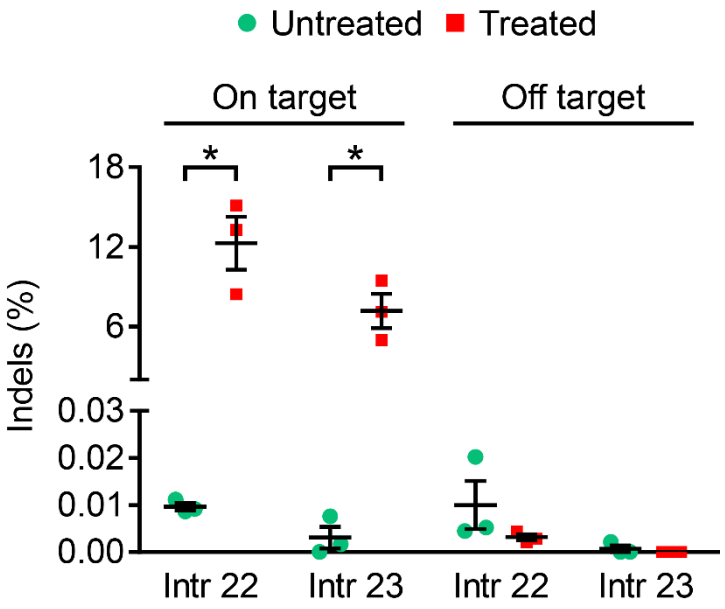

Fig. S14. Quantification of indels by deep sequencing in study #2. Deep sequencing was performed on both the target sites and predicted off-target sites in untreated and CRISPR treated mdx mice. Significant on-target editing was observed for both gRNAs only in CRISPR treated mdx mice. Off-target editing was not detected with either gRNA (n=3). Multiple t-tests was used for statistical analysis. Asterisk, statistically significant ($p<0.05$).

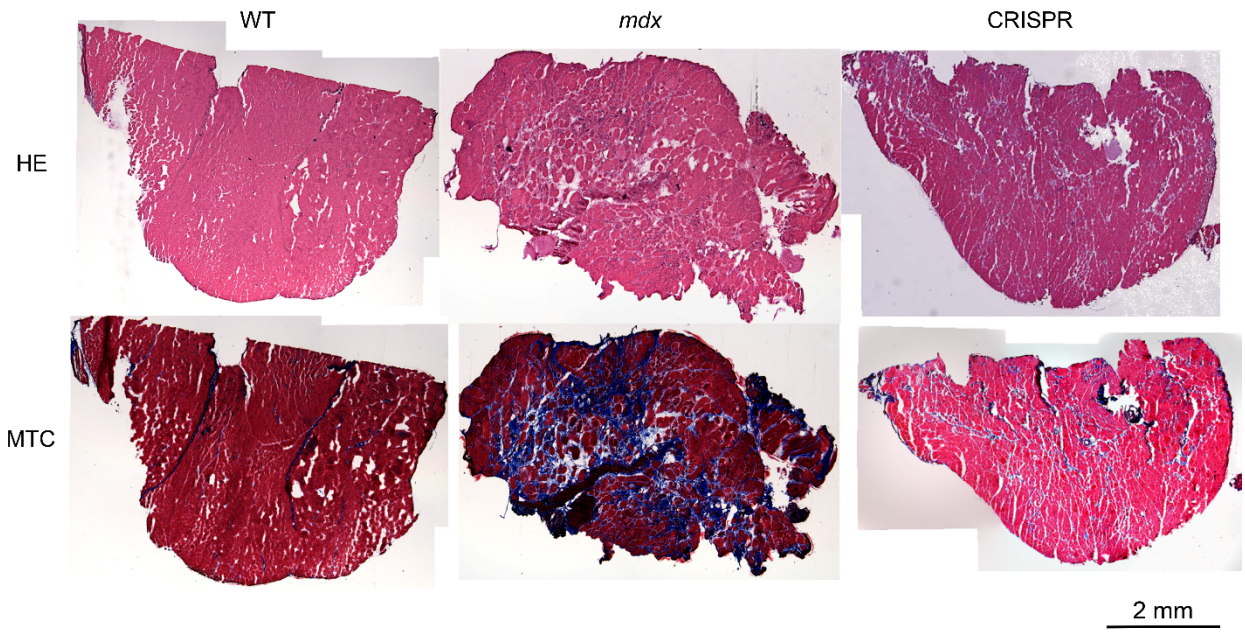

Fig. S15. Evaluation of skeletal muscle histology and fibrosis in study #2. Representative full-view images of HE and Masson trichrome (MTC) staining of the gastrocnemius from normal BL10 (WT), untreated mdx and CRISPR treated mdx mice.

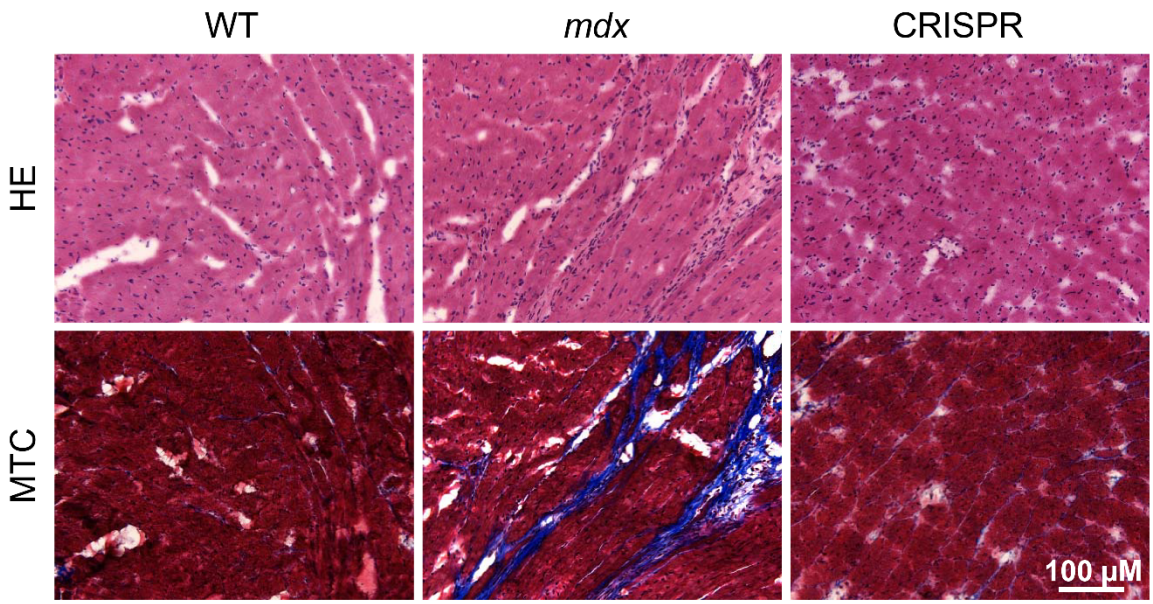

Fig. S16. Evaluation of cardiac histology and fibrosis in study #2. Representative high-power images of HE and Masson trichrome (MTC) staining of the heart from normal BL10 (WT), untreated mdx and CRISPR treated mdx mice.

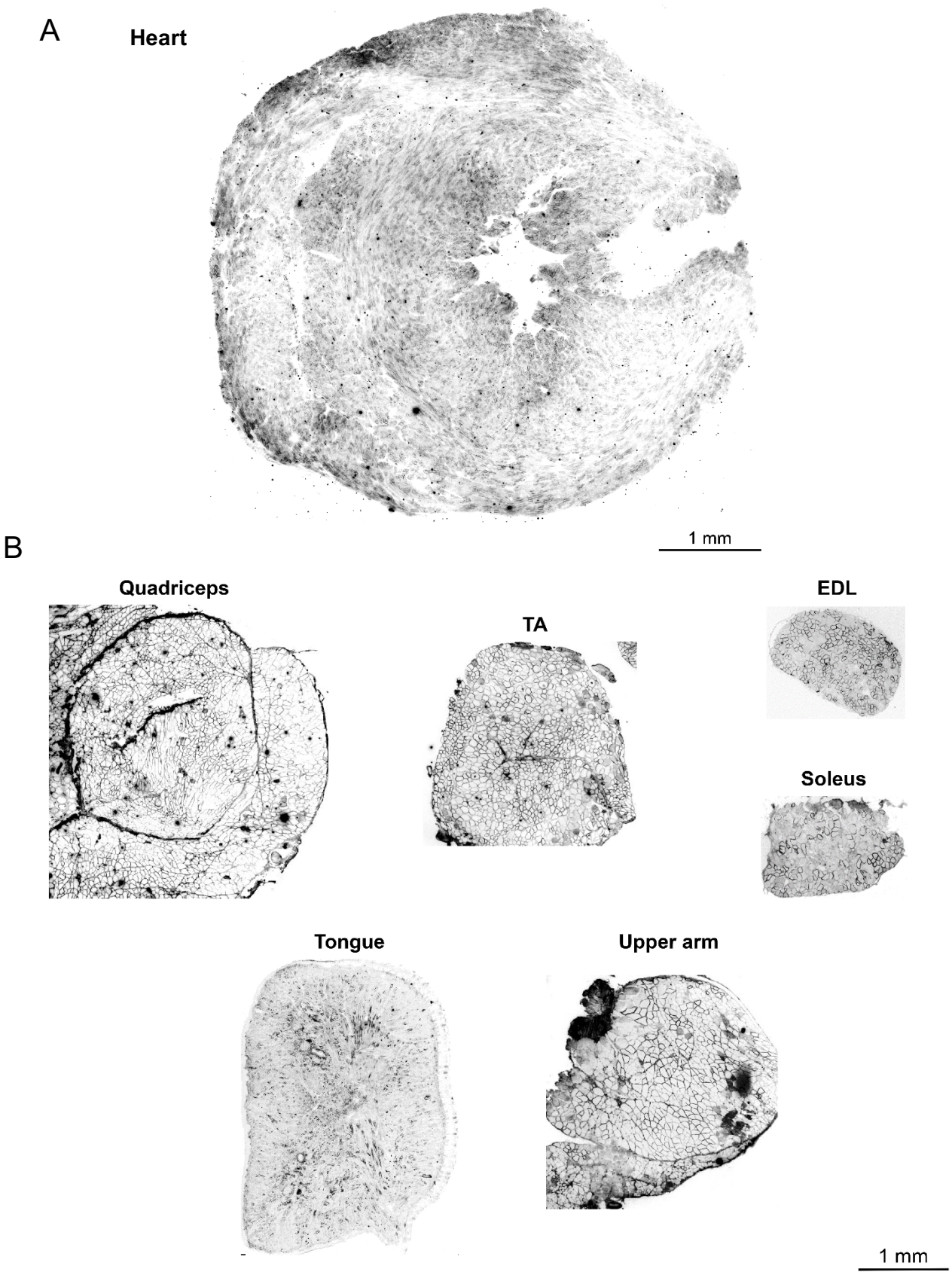
A
Heart
1 mm
B
Quadriceps
TA
EDL
Soleus
Tongue
Upper arm
1 mm

Fig. S17. Representative dystrophin immunofluorescence staining in study #3. A, Representative full-view dystrophin staining images of the heart. **B,** Representative high power dystrophin staining images from the quadriceps (Quadro), upper arm muscle, extensor digitorum longus (EDL), tibialis anterior (TA), soleus and tongue.

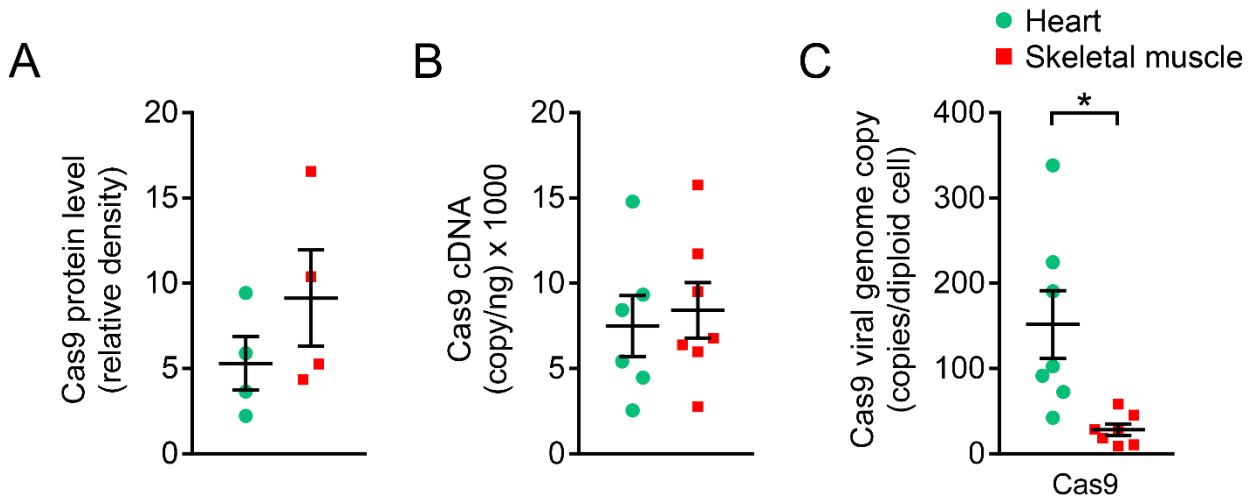

Fig. S18. Evaluation of Cas9 protein, Cas9 transcript and Cas9 AAV genome copy number in study #3. The Cas9 protein was examined by quantitative western blot (n=4 for each tissue). The Cas9 cDNA copy number was determined by digital droplet PCR (n=6 for heart and n=7 for skeletal muscle). The Cas9 AAV genome copy number was determined by TaqMan PCR (n=7 for each tissue). Mann-Whitney test was used for statistical analysis. Statistically significant ($p<0.05$).

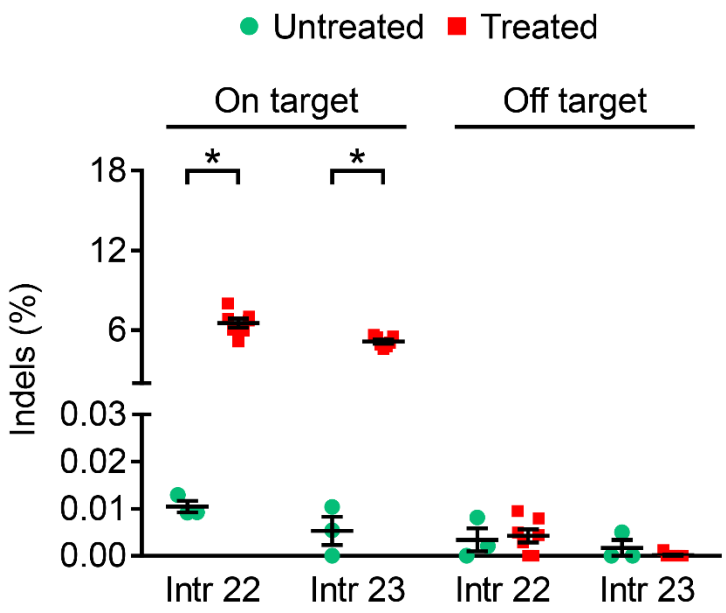

Fig. S19. Quantification of indels by deep sequencing in study #3. Deep sequencing was performed on both the target sites and predicted off-target sites in untreated and CRISPR treated mdx mice. Significant on-target editing was observed for both gRNAs only in CRISPR treated mdx mice. Off-target editing was not detected with either gRNA (n=3 for untreated and n=7 for treated). Multiple t-tests were used for statistical analysis. Asterisk, statistically significant ($p<0.05$).

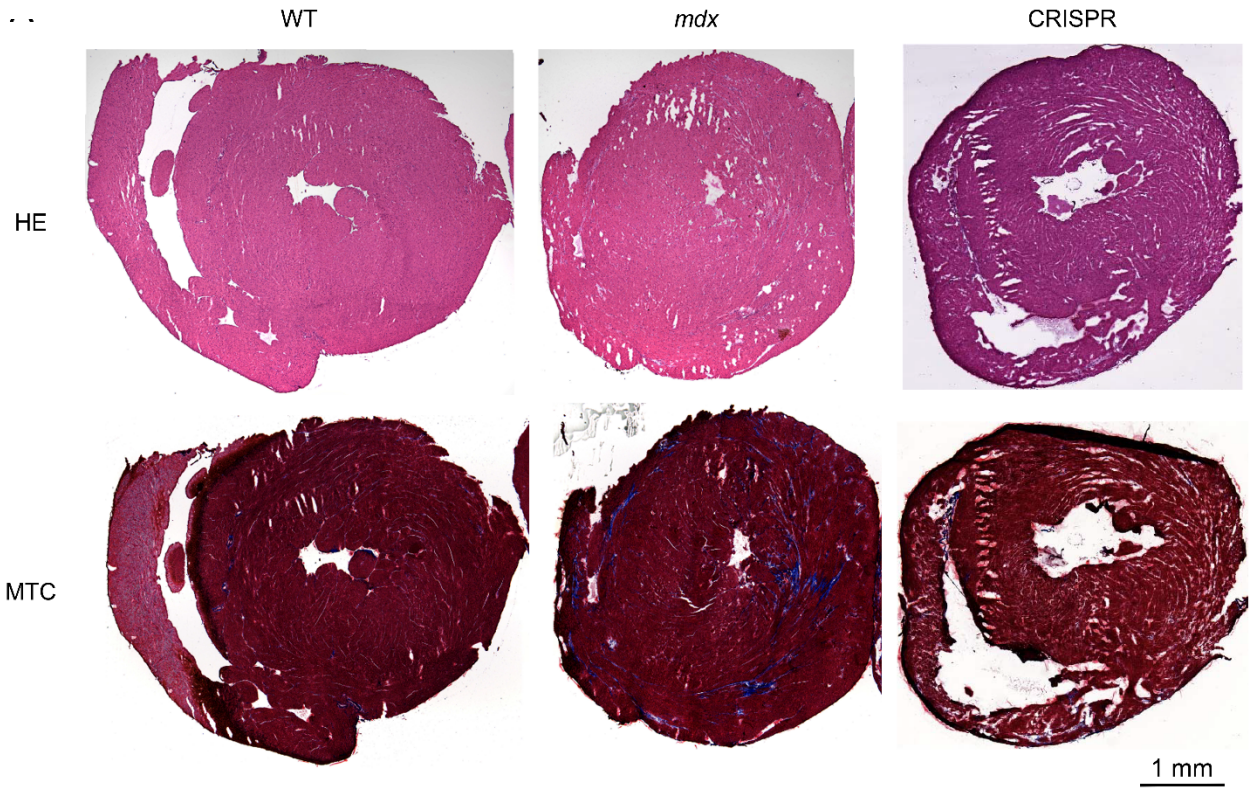

Fig. S20. Evaluation of cardiac histology and fibrosis in study #3. Representative full-view images of HE and Masson trichrome (MTC) staining of the heart from normal BL10 (WT), untreated mdx and CRISPR treated mdx mice.

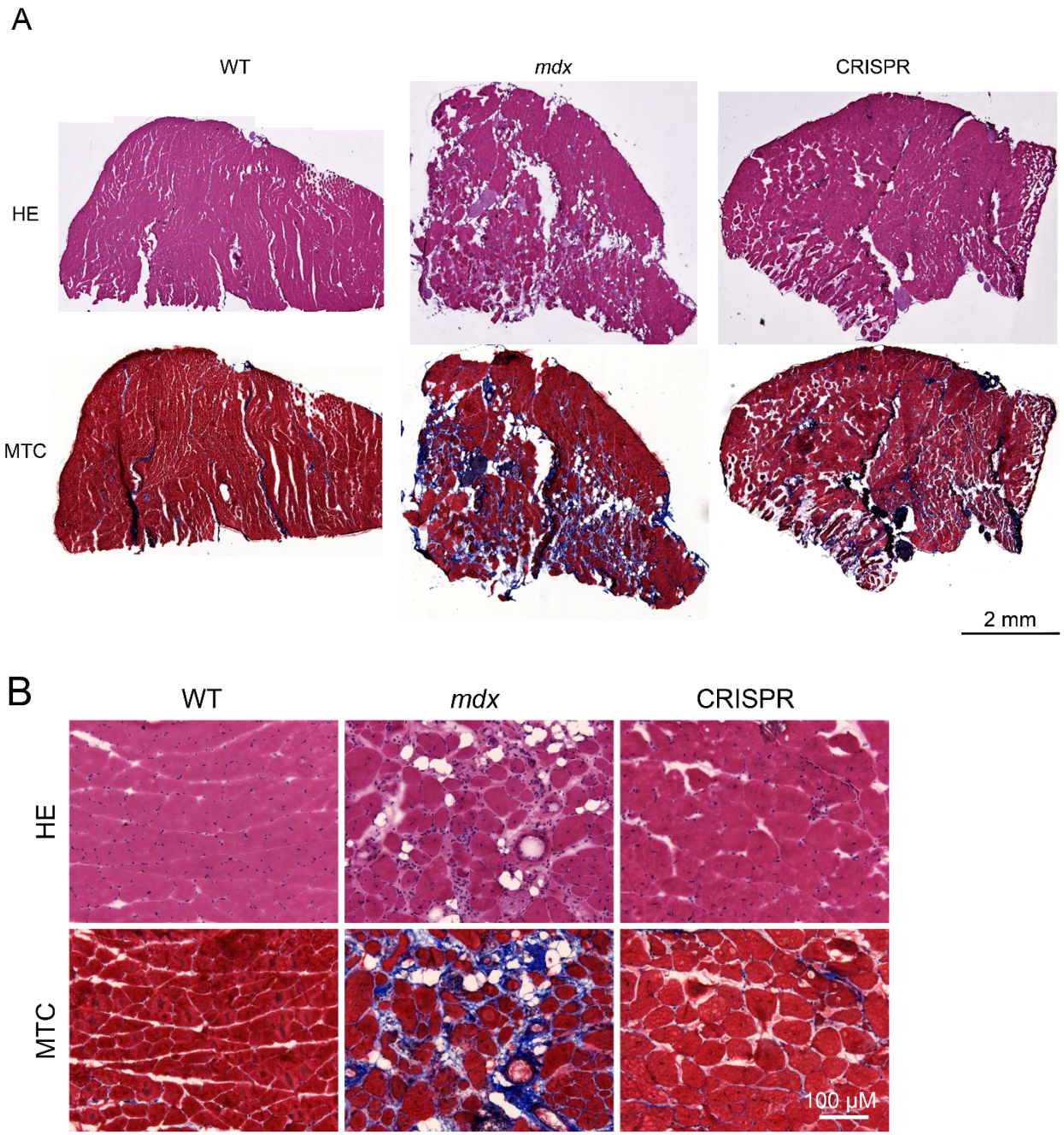

Fig. S21. Evaluation of skeletal muscle histology and fibrosis in study #3. A, Representative full-view images of HE and Masson trichrome (MTC) staining of the gastrocnemius from normal BL10 (WT), untreated mdx and CRISPR treated mdx mice. **B,** Representative high-power

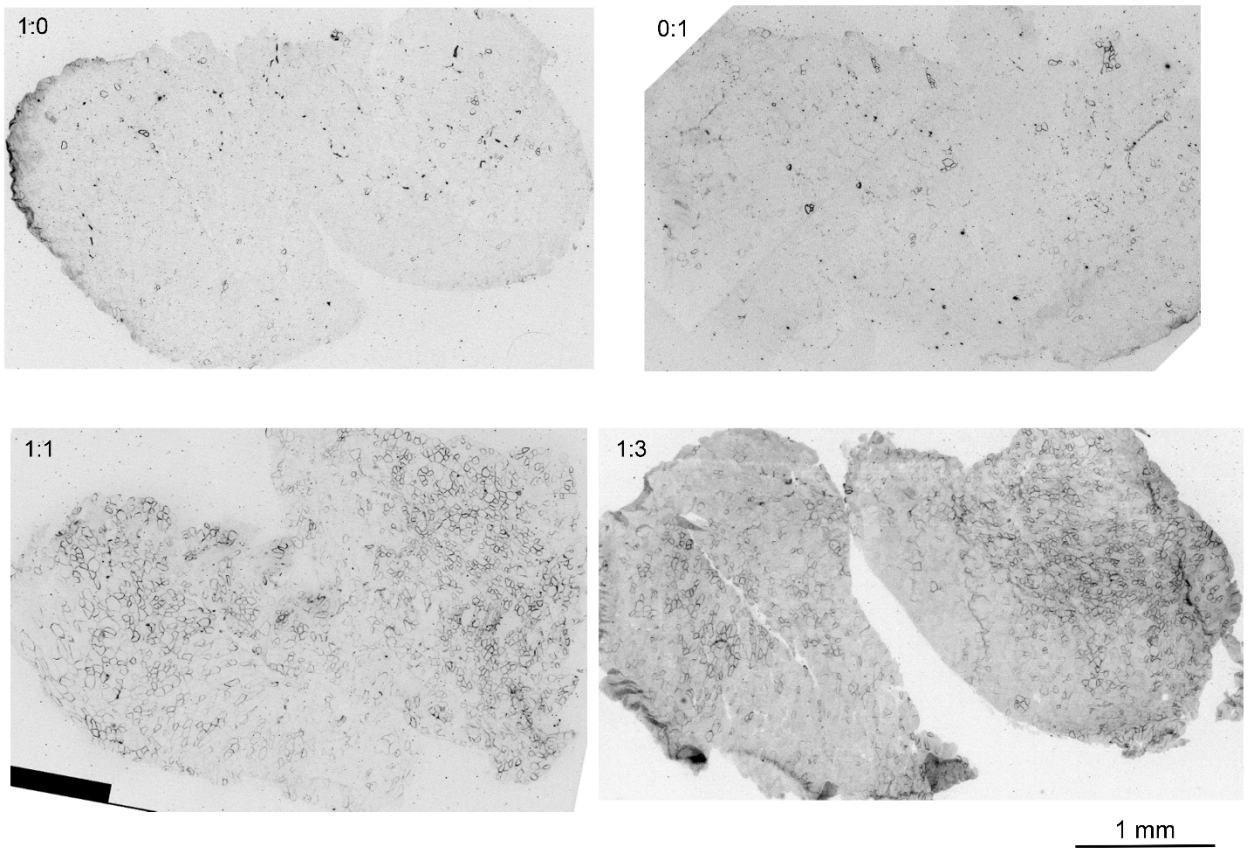

images of HE and MTC staining of the gastrocnemius from normal, untreated mdx and CRISPR treated mdx mice.

Fig. S22. Representative full-view dystrophin immunofluorescence staining images in local injection study. The Cas9 and gRNA AAV-9 vectors were injected to the tibias anterior (TA) muscle at the ratio of 1:0 (Cas9 vector only), 0:1 (gRNA vector only), 1:1 (equal amount of the Cas9 and gRNA vectors) and 1:3 (three-fold more gRNA vector). Representative full-view photomicrographs from each injection condition are shown. Each panel contains two TA muscle sections.

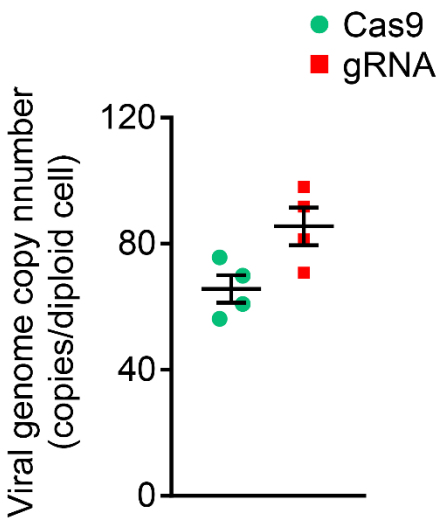

Fig. S23. AAV genome copy number quantification in the local injection study described by Nelson et al in 2016. The AAV genome copy number was quantified using muscle tissues collected in our previously published paper (Nelson et al *Science* 351:403-7,2016). Specifically, Cas9 and gRNA AAV-8 vectors were injected to the tibias anterior (TA) muscle of 6-week-old mdx mice at the dose of 7 x 10^{11} vg/vector/muscle. Muscle was collected at two months after injection. The AAV genome copy number was determined by TaqMan PCR using method described in this manuscript. Similar genome copy numbers were observed for the Cas9 and gRNA vectors. There was no preferential depletion of the gRNA AAV genome (n=4 for each vector). Mann-Whitney test was used for statistical analysis.

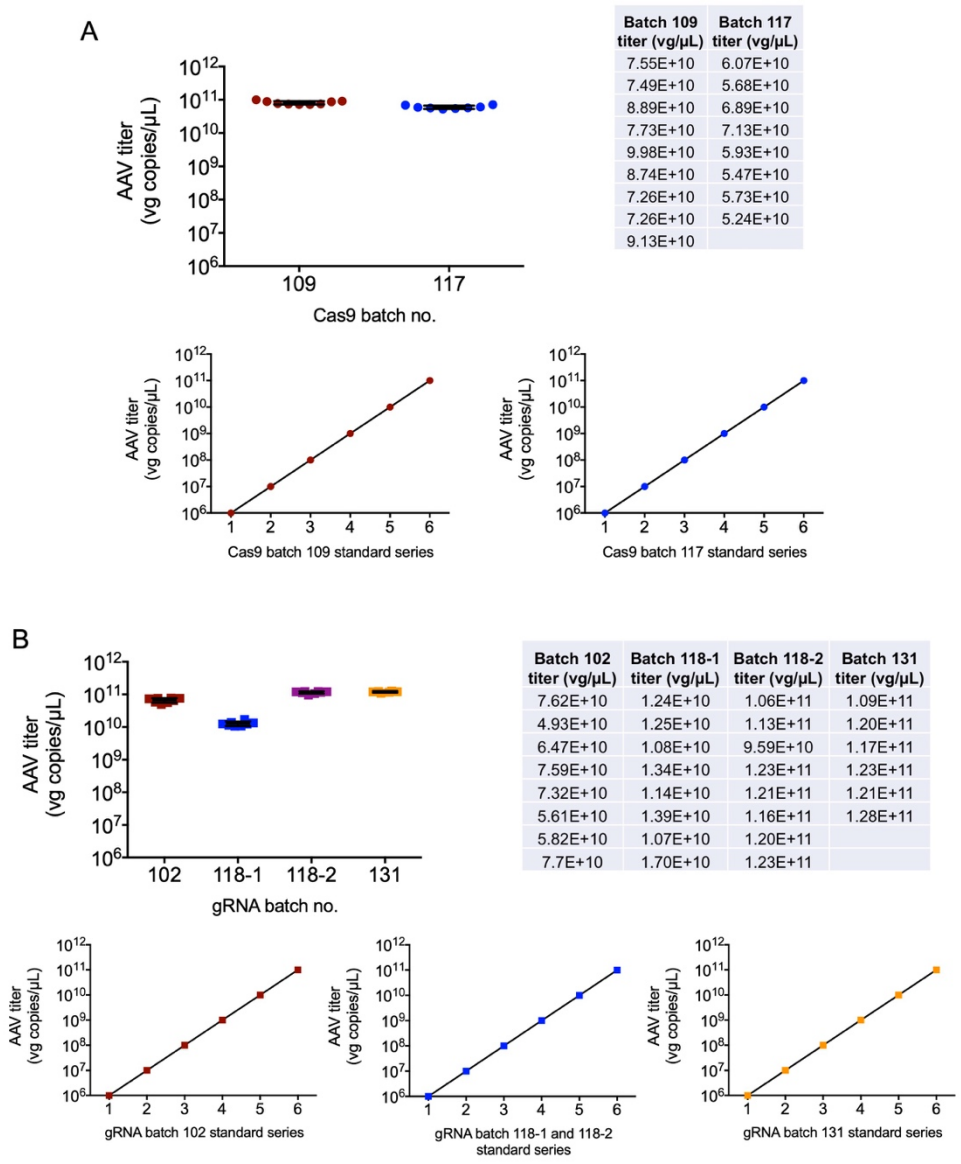

Batch 109 titer (vg/µL)	Batch 117 titer (vg/µL)
7.55E+10	6.07E+10
7.49E+10	5.68E+10
8.89E+10	6.89E+10
7.73E+10	7.13E+10
9.98E+10	5.93E+10
8.74E+10	5.47E+10
7.26E+10	5.73E+10
7.26E+10	5.24E+10
9.13E+10	

Batch 102 titer (vg/µL)	Batch 118-1 titer (vg/µL)	Batch 118-2 titer (vg/µL)	Batch 131 titer (vg/µL)
7.62E+10	1.24E+10	1.06E+11	1.09E+11
4.93E+10	1.25E+10	1.13E+11	1.20E+11
6.47E+10	1.08E+10	9.59E+10	1.17E+11
7.59E+10	1.34E+10	1.23E+11	1.23E+11
7.32E+10	1.14E+10	1.21E+11	1.21E+11
5.61E+10	1.39E+10	1.16E+11	1.28E+11
5.82E+10	1.07E+10	1.20E+11	
7.7E+10	1.70E+10	1.23E+11	

Fig. S24. Titration of the SaCas9 and gRNA AAV vectors used in the study. A total of two independent batches of the SaCas9 vector and four independent batches of the gRNA vector were made for the study. Each batch was titrated independently by qPCR. At each PCR reaction, known amount plasmid DNA were used to generate the standard curve. Different batches of the same vector were combined, aliquoted and stored in a -80ºC freezer. Freshly

thawed aliquots were used for mouse injection. Leftover was discarded and not re-used. Titration results from each batch of the AAV preparation are shown in this Figure. **A,** Titration results for the SaCas9 vector. For batch 109, we did nine qPCR reactions and the average of these was used as the batch 109 titer (8.23×10^{10} vg/µl). For batch 117, we did eight qPCR reactions and the average of these was used as the batch 117 titer (6.02×10^{10} vg/µl). **B,** Titration results for the gRNA vector. For batch 102, we did eight qPCR reactions and the average of these was used as the batch 102 titer (6.63×10^{10} vg/µl). For batch 118-1, we did eight qPCR reactions and the average of these was used as the batch 118-1 titer (1.28×10^{10} vg/µl). For batch 118-2, we did eight qPCR reactions and the average of these was used as the batch 118-2 titer (1.15×10^{11} vg/µl). Please note, batch 118-1 and 118-2 titration were performed in the same qPCR plate. Hence these two batches shared the same standard curve. For batch 131, we did six qPCR reactions and the average of these was used as the batch 131 titer (1.20×10^{11} vg/µl).

Table S1. Summary of three systemic AAV CRISPR studies described in this manuscript

	n	Sex	Age at injection (m)	Body weight at injection (g)	AAV vector (vg/mouse)		AAV vector (vg/kg)	
					Cas9	gRNA	Cas9	gRNA
Study #1	6	male	1.54 ± 0.02	22.6 ± 0.43	7.20E+12	3.63E+12	3.19E+14	1.61E+14
Study #2	6	male	1.56 ± 0.07	21.5 ± 0.55	1.00E+13	3.00E+13	4.61E+14	1.38E+15
Study #3	8	female	1.48 ± 0.05	16.1 ± 0.68	1.00E+13	3.00E+13	6.07E+14	1.82E+15

Table S2. Anatomic properties of mice harvested at 18 months in study #1

	WT	mdx	CRISPR
n	15	18	5
Age (m)	18.77 ± 0.35	18.85 ± 0.32	18.90 ± 0.05
BW (g)	33.33 ± 0.63	31.58 ± 0.95	23.74 ± 0.42 #
HW (mg)	136.26 ± 2.45	132.68 ± 3.78	122.62 ± 8.71
VW (mg)	129.09 ± 2.46	122.67 ± 3.03	116.60 ± 8.40
TW (mg)	42.03 ± 1.05	52.84 ± 2.92 *	44.45 ± 2.59
HW/BW (mg/g)	4.11 ± 0.11	4.30 ± 0.12	5.15 ± 0.29 #
TW/BW (mg/g)	1.26 ± 0.03	1.61 ± 0.14	1.87 ± 0.08 *
HW/TW (mg/g)	3.28 ± 0.12	2.68 ± 0.17 *	2.77 ± 0.16
VW/BW (mg/g)	3.89 ± 0.11	3.98 ± 0.12	4.90 ± 0.28 #
VW/TW (mg/g)	3.10 ± 0.11	2.47 ± 0.15 *	2.63 ± 0.16

*, Significantly different from WT

#, Significantly different from WT and mdx

Abbreviations: BW, body weight; HW, heart weight; TW, tibialis muscle weight; VW, ventricle weight.

Statistical analysis was done using One-way ANOVA.

Table S3. ECG results from study #1

	WT	mdx	CRISPR
n	18	11	5
Age	19.26 ± 0.44	19.34 ± 0.71	18.78 ± 0.04
Heart rate (bpm)	572.93 ± 8.96	617.86 ± 14.33 *	584.44 ± 10.28
PR Interval (ms)	40.18 ± 0.65	34.97 ± 1.14 *	38.17 ± 1.05
QRS Duration (ms)	8.09 ± 0.19 #	9.71 ± 0.58	10.33 ± 0.34
QTc (ms)	20.12 ± 0.43	27.77 ± 0.74 †	19.82 ± 0.66
Cardiomyopathy Index	0.7 ± 0.02	1.4 ± 0.17 †	0.69 ± 0.03
Q amplitude (μV)	-32.06 ± 4.68	-60.95 ± 35.89	-143.15 ± 31.90 *

*, Significantly different from WT

#, Significantly different from mdx and CRISPR

†, Significantly different from WT and CRISPR

Statistical analysis was done using One-way ANOVA.

Table S4. Hemodynamic results from study #1

	WT	mdx	CRISPR
n	15	9	5
Age	19.72 ± 0.57	19.68 ± 0.92	18.94 ± 0.02
End systolic volume (µL)	8.88 ± 1.27	11.01 ± 3.37	8.73 ± 2.17
End diastolic volume (µL)	30.02 ± 1.78 #	20.78 ± 2.72	20.26 ± 2.37
Max pressure (mmHg)	103.62 ± 2.08 #	88.00 ± 3.95	87.07 ± 7.65
Ejection fraction (%)	75.03 ± 3.57	63.86 ± 8.10	63.40 ± 6.98
Stroke volume (µL)	23.47 ± 1.41 #	12.83 ± 0.95	12.73 ± 1.27
Cardiac output (mL/min)	14585.05 ± 885.44 #	7646.23 ± 542.72	7480.39 ± 595.40
dP/dt max (KmmHg /sec)	13163.20 ± 446.52 #	9940.56 ± 990.41	9438.80 ± 483.43
dP/dt min (KmmHg /sec)	-12551.40 ± 677.10 #	-8507.67 ± 666.57	-8450.60 ± 568.90
Tau (ms)	6.30 ± 0.32	7.47 ± 0.55	9.55 ± 1.45*

*, Significantly different from WT

#, Significantly different from mdx and CRISPR

Statistical analysis was done using One-way ANOVA.

Table S5. Anatomic properties of the EDL muscle in study #2

Strain	n	EDL weight (mg)	Lo (mm)	CSA (mm^2)
WT	7	12.62 ± 0.29	13.16 ± 0.05	2.06 ± 0.05
mdx	12	16.13 ± 0.64 #	13.99 ± 0.11 #	2.48 ± 0.09 #
CRISPR	6	12.14 ± 0.85	13.40 ± 0.15	1.95 ± 0.14

Significantly different from BL10 and CRISPR
EDL, Extensor digitorum longus muscle
Lo, Optimal muscle length
CSA, Muscle cross-sectional area

Statistical analysis was done using One-way ANOVA.

Table S6. Anatomic properties of mice in study #3

	WT	mdx	CRISPR
n	20	20	8
Age (m)	18.2 ± 0.44	18.74 ± 0.45	18.53 ± 0.07
BW (g)	30.2 ± 0.91 †	22.36 ± 0.39	22.43 ± 0.88
HW (mg)	115.8 ± 1.99 †	108 ± 1.76	99.20 ± 3.99
VW (mg)	109.9 ± 1.88 †	102 ± 1.62	95.23 ± 3.60
TW (mg)	38.51 ± 0.70	42.78 ± 2.18	46.89 ± 0.56 *
HW/BW (mg/g)	3.88 ± 0.10 †	4.8 ± 0.07	4.44 ± 0.15
HW/TW (mg/g)	3.1 ± 0.06 †	2.61 ± 0.15	2.12 ± 0.098 #
VW/BW (mg/g)	3.69 ± 0.10 †	4.54 ± 0.07	4.27 ± 0.14
VW/TW (mg/g)	2.86 ± 0.05 †	2.4 ± 0.12	2.04 ± 0.09

*, Significantly different from WT

†, Significantly different from mdx and CRISPR

#, Significantly different from mdx

Abbreviations: BW, body weight; HW, heart weight; TW, tibialis muscle weight; VW, ventricle weight.

Statistical analysis was done using One-way ANOVA.

Table S7. ECG results from study #3

	WT	mdx	CRISPR
n	18	15	8
Age	18.36 ± 0.55	18.87 ± 0.48	18.28 ± 0.04
Heart rate (bpm)	557.74 ± 16.22	615.00 ± 14.78*	586.45 ± 9.05
PR Interval (ms)	40.96 ± 0.80	33.73 ± 0.80*	36.85 ± 1.13
QRS Duration (ms)	8.68 ± 0.23	10.17 ± 0.34*	9.54 ± 0.59
QTc (ms)	18.81 ± 0.57#	25.52 ± 1.14	22.2 ± 1.32
Cardiomyopathy Index	0.66 ± 0.04	1.08 ± 0.05*	0.89 ± 0.06
Q amplitude (μV)	-29.27 ± 5.58	-96.15 ± 18.18*	-47.25 ± 14.55

*, Significantly different from WT

#, Significantly different from mdx and CRISPR

Statistical analysis was done using One-way ANOVA (heart rate and QTc) or Kruskal-Wallis test (PR, QRS, cardiomyopathy index and Q amplitude).

Table S8. Hemodynamic results from study #3

	WT	mdx	CRISPR
n	18	15	7
Age	17.99 ± 0.41	18.82 ± 0.49	18.29 ± 0.04
End diastolic volume (µL)	20.90 ± 1.72	23.27 ± 1.90	19.91 ± 2.90
Max pressure (mmHg)	101.73 ± 1.44 #	86.47 ± 5.00	91.50 ± 2.57
Stroke volume (µL)	16.96 ± 1.12	10.17 ± 0.61*	12.95 ± 1.12
Cardiac output (mL/min)	10218.58 ± 651.91	6002.17 ± 327.11*	7462.68 ± 725.59
dP/dt max (KmmHg /sec)	13571.17 ± 541.32	10402.07 ± 958.94*	11047.29 ± 1036.77
dP/dt min (KmmHg /sec)	-11863.11 ± 498.94	-9414.93 ± 821.74*	-11363.86 ± 894.92
Tau (ms)	7.48 ± 0.55	8.42 ± 0.36	6.87 ± 0.47

*, Significantly different from WT

#, Significantly different from mdx and CRISPR

Statistical analysis was done using One-way ANOVA (ESV, SV, dP/dt max, dP/dt min) or Kruskal-Wallis test (Max P, cardiac output, Tau).

Table S9. Summary of the local AAV CRISPR study

Vector ratio (Cas9:gRNA)	n	Cas9 vector (vg/muscle)	gRNA vector (vg/muscle)
Un-injected	6	0.00E+00	0.00E+00
(0:1)	4	0.00E+00	1.00E+11
(1:0)	4	1.00E+11	0.00E+00
(1:1)	4	1.00E+11	1.00E+11
(1:3)	4	1.00E+11	3.00E+11

Table S10. TaqMan primers and probes used in viral genome and dystrophin transcript quantifications

Target	Forward primer	Reverse primer	TaqMan probe
SaCAS9	CGCACAGAAGATGATCAATGAGATG	TTCGGATAATCTCTTCAATGCGTTCA	TTGGTCTGCCGGTTTC
gRNA	GAGCGCACCATCTTCTTCAAG	TGTCGCCCTCGAACTTCAC	ACGACGGCAACTACA
Exon 22-23	CTGAATATGAAATAATGGAGGAGAGACTCG	AGTTGAAGCCATTTTGTTGCTCTTTC	CAGAGCCTGTAATTTC
Exon 22-24	AGGAGAGACTCGGGAAATTACAGAA	GGCAGGCCATTCCTCTTTCA	CAGCCATCCATTTCTG
Exon 24-25	GGGATGCTGAAATCCTGAAAAAACA	TTCTGCCCACCTTCATTAACACTATT	TCAAACAATGCAGACTTTT

Table S11. Primers used for deep sequencing analysis

Primer	Sequence
1	TCGTCGGCAGCGTCAGATGTGTATAAGAGACAG tttctgtctaaatataatatgccctgt
2	GTCTCGTGGGCTCGGAGATGTGTATAAGAGACAG gcagagcctcaaaattaaatagaag
3	TCGTCGGCAGCGTCAGATGTGTATAAGAGACAG gagctcatcctctttcatgct
4	GTCTCGTGGGCTCGGAGATGTGTATAAGAGACAG gaaggaggaacaggcaggag
5	TCGTCGGCAGCGTCAGATGTGTATAAGAGACAG aaagttgttagagcctgctcatt
6	GTCTCGTGGGCTCGGAGATGTGTATAAGAGACAG tttagtagacggaagaaagctca
7	TCGTCGGCAGCGTCAGATGTGTATAAGAGACAG tggatatcctcctgggaatg
8	GTCTCGTGGGCTCGGAGATGTGTATAAGAGACAG gcctcaactggaaactgagc
9	AATGATACGGCGACCACCGAGATCTACACTCGTCGGCAGCGTC
10	CAAGCAGAAGACGGCATACGAGAT NNNNNN GTCTCGTGGGCTCGG

Uppercase, specific for Illumina sequencing

Lowercase, genome specific sequence

NNNNNN, barcodes used in the sequencing